

Modern Physics Letters A
© World Scientific Publishing Company

IMPLEMENTATION OF THE ATLAS-SUSY-2018-04 ANALYSIS IN THE MADANALYSIS 5 FRAMEWORK

Jongwon Lim

Department of Physics, Hanyang University, Seoul 04763, Republic of Korea

Chih-Ting Lu

School of Physics, KIAS, Seoul 02455, Republic of Korea

Jae-hyeon Park

School of Physics, KIAS, Seoul 02455, Republic of Korea

Jiwon Park

Department of Physics, Hanyang University, Seoul 04763, Republic of Korea

Received (Day Month Year)

Revised (Day Month Year)

We present the MADANALYSIS 5 implementation and validation of the ATLAS-SUSY-2018-04 search. This ATLAS analysis targets the search for direct stau production in events with two hadronic tau leptons and probes 139 fb^{-1} of LHC proton-proton collisions at a center-of-mass energy of 13 TeV. The validation of our reimplementation relies on a comparison of our cutflow predictions with the auxiliary table of official ATLAS results in the context of two supersymmetry-inspired simplified benchmark models in which the Standard Model is extended by a neutralino and a stau decaying into a tau lepton and a neutralino.

Keywords: supersymmetry; stau; hadronic tau lepton.

1. Introduction

In this note, we describe the validation of the implementation, in MADANALYSIS 5 framework,^{1–4} of the ATLAS-SUSY-2018-04 search⁵ for direct stau production in two hadronic $\tau + E_T^{\text{miss}}$ events. This process is illustrated by the representative Feynman diagram of Fig. 1. This analysis focuses on LHC proton-proton collisions at a center-of-mass energy of 13 TeV and an integrated luminosity of 139 fb^{-1} .

For the validation of our reimplementation, we have focused on the sector of sparticles with only electroweak interactions. The lightest neutralino ($\tilde{\chi}_1^0$) is taken as the lightest supersymmetric particle (LSP). The stau-left ($\tilde{\tau}_L$) and stau-right ($\tilde{\tau}_R$) are assumed to be mass degenerate without mixing. Therefore the gauge eigenstates ($\tilde{\tau}_L, \tilde{\tau}_R$) coincide with the mass eigenstates ($\tilde{\tau}_1, \tilde{\tau}_2$). Furthermore, in order to suppress

2 Jongwon Lim, Chih-Ting Lu, Jae-hyeon Park, and Jiwon Park

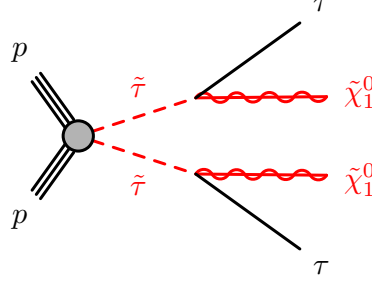


Fig. 1. The Feynman diagram for the process $pp \rightarrow \tilde{\tau}\tilde{\tau} \rightarrow \tilde{\chi}_1^0\tilde{\chi}_1^0\tau\tau$.

other decay modes of stau, the masses of all charginos and neutralinos are set to 2.5 TeV except for the $\tilde{\chi}_1^0$. Hence, the single kinematically allowed decay mode of stau is

$$\tilde{\tau} \rightarrow \tilde{\chi}_1^0 \tau \quad (1)$$

2. Description of the analysis

This analysis targets a final state containing two hadronic tau leptons with a certain amount of missing transverse energy. The kinematics of di- $\tau + E_T^{miss}$ system is used to reduce the contributions from Standard Model backgrounds. First, all the objects are reconstructed and defined. Then a sequence of event selections for the signal final state is applied.

2.1. Object definitions

Jets are reconstructed by means of the anti- k_t algorithm⁷ with a radius parameter set to $R = 0.4$. This analysis focuses on jets whose transverse momentum p_T^j and pseudorapidity η^j fulfill

$$p_T^j > 20\text{GeV} \quad \text{and} \quad |\eta^j| < 2.8. \quad (2)$$

Moreover, the selected jets are tagged as originating from the fragmentation of a b -quark with

$$p_T^b > 20\text{GeV} \quad \text{and} \quad |\eta^b| < 2.5. \quad (3)$$

A working point with the average b -tagging efficiency of 77% is used. This working point corresponds to a c -jet and light-jet rejection of 4.9 and 110, respectively.

Electron candidates are required to have a transverse momentum p_T^e and pseudorapidity η^e obeying

$$p_T^e > 17\text{GeV} \quad \text{and} \quad |\eta^e| < 2.47. \quad (4)$$

Furthermore, all electron candidates are required to have both track and calorimeter isolations. The condition of the track isolation is

$$\sum p_{T,\text{tracks}}/p_T^e < 0.15 \quad \text{with} \quad \Delta R = \min(10\text{GeV}/p_T^e, 0.2), \quad (5)$$

the condition of the calorimeter isolation is

$$\sum E_{T,\text{calorimeter}}/p_T^e < 0.2 \quad \text{with} \quad \Delta R = 0.2, \quad (6)$$

and for high transverse momentum electron,

$$\sum E_{T,\text{tracks}} < \max(0.015 \times p_T^e, 3.5\text{GeV}) \quad \text{with} \quad \Delta R = 0.2 \quad \text{if} \quad p_T^e > 200\text{GeV}. \quad (7)$$

Muon candidate definition is similar, although with slightly looser thresholds,

$$p_T^\mu > 14\text{GeV} \quad \text{and} \quad |\eta^\mu| < 2.7, \quad (8)$$

The condition of the track isolation is

$$\sum p_{T,\text{tracks}}/p_T^\mu < 0.15 \quad \text{with} \quad \Delta R = \min(10\text{GeV}/p_T^\mu, 0.3), \quad (9)$$

and the condition of the calorimeter isolation is

$$\sum E_{T,\text{tracks}}/p_T^\mu < 0.3 \quad \text{with} \quad \Delta R = 0.2. \quad (10)$$

Tau lepton candidates are reconstructed with one or three associated charged pion tracks (prongs). For 1-prong (3-prong) τ lepton candidates, the signal efficiencies are 75% and 60% for the *medium* working points. Due to the technical restriction, the *tight* working point efficiencies are directly taken from the official ATLAS cutflow table. The baseline tau lepton candidates are required to have

$$p_T^\tau > 50(40)\text{GeV} \quad \text{and} \quad |\eta^\tau| < 2.5 \quad (11)$$

for the leading (subleading) ones and the transition region between the barrel and endcap calorimeters ($1.37 < |\eta^\tau| < 1.52$) is excluded.

Finally, some overlap removal conditions are in order which are consistent with the analysis code provided in HEPData.⁶ Electron is removed if $\Delta R(e, e) < 0.05$. Tau lepton is removed if $\Delta R(\tau, e/\mu) < 0.2$. Electron is removed if $\Delta R(e, \mu) < 0.01$. Jet is removed if $\Delta R(j, e/\mu) < 0.2$, and then electron or muon is removed if $\Delta R(e/\mu, j) < 0.4$, and jet is removed if $\Delta R(j, \tau) < 0.4$.

2.2. Event selection

All events are required to pass either an *asymmetric di- τ* trigger for the low stau mass region (SR-lowMass) or a combined *di- τ + E_T^{miss}* ($E_T^{\text{miss}} > 150$ GeV) trigger for the high stau mass region (SR-highMass) (**Trigger and offline cuts**). The trigger efficiencies about 80% are applied in our recasting with the following offline p_T thresholds for the leading (subleading) tau lepton candidates in Table 1.

Then events with exactly two *medium* tau lepton candidates with opposite-sign electric charge (OS) are selected. Then, *b*-jet veto is applied to reject events from

4 Jongwon Lim, Chih-Ting Lu, Jae-hyeon Park, and Jiwon Park

Table 1. Offline p_T thresholds for the leading (subleading) tau lepton candidates of *asymmetric* $di\text{-}\tau$ and $di\text{-}\tau + E_T^{miss}$ triggers with efficiencies about 80%.

Year	<i>asymmetric</i> $di\text{-}\tau$	$di\text{-}\tau + E_T^{miss}$
2015-2017	95(60) GeV	50(40) GeV
2018	95(75) GeV	75(40) GeV

top quark associated processes. Also, the events with additional light lepton (muon or electron) are rejected. The reconstructed invariant mass of the two leading tau lepton candidates, $m(\tau_1, \tau_2)$, larger than 120 GeV is required for removing tau lepton pair from low-mass resonances, Z boson, and Higgs boson events (Z/H veto).

In SR-lowMass region, values of $75 < E_T^{miss} < 150$ GeV are required for SR-lowMass to increase signal sensitivity. Also, two selected tau leptons are required to be tight tagged. The selection efficiency of two taus passing the *tight* working point on top of two medium tagged tau leptons is taken from official ATLAS cutflow table as a ratio of raw number of event before and after applying cut ($p_{tight} \simeq 0.70$), and the tight tagging efficiency is then applied as a probability per tau lepton by a square root of the efficiency ($\sqrt{p_{tight}} \simeq 0.84$). On the other hand, in SR-highMass region, the tight tagging efficiency is applied in the same manner as SR-lowMass region, but allowing at least one of two tau leptons passing the tight selection ($p_{tight} + 2\sqrt{p_{tight}}(1 - \sqrt{p_{tight}}) \simeq 0.97$).

The *stransverse mass* m_{T2} variable is defined as^a

$$m_{T2} = \min_{\mathbf{q}_T} [\max(m_{T,\tau_1}(\mathbf{p}_{T,\tau_1}, \mathbf{q}_T), m_{T,\tau_2}(\mathbf{p}_{T,\tau_2}, \mathbf{p}_T^{miss} - \mathbf{q}_T))], \quad (12)$$

where \mathbf{p}_{T,τ_1} and \mathbf{p}_{T,τ_2} are the transverse momenta of the two tau lepton candidates, and the transverse momentum vector of one of the invisible particle, \mathbf{q}_T , is chosen to minimize the larger of the two transverse mass m_{T,τ_1} and m_{T,τ_2} . The transverse mass m_T is defined by

$$m_T(\mathbf{p}_T, \mathbf{q}_T) = \sqrt{2(p_T q_T - \mathbf{p}_T \cdot \mathbf{q}_T)}. \quad (13)$$

A lower bound on the m_{T2} will be imposed to reduce contributions from $t\bar{t}$ and WW events. Finally, the two tau lepton candidates are required to satisfy $\Delta R(\tau_1, \tau_2) < 3.2$, $|\Delta\phi(\tau_1, \tau_2)| > 0.8$ and $m_{T2} > 70$ GeV to further suppress contributions from SM backgrounds.

3. Validation

3.1. Event generation

In order to validate our analysis, we rely on the MSSM UFO model file⁸ from Feynrules model database.⁹ Two benchmark points with masses $m(\tilde{\tau}, \tilde{\chi}_1^0) = (120, 1)\text{GeV}$

^aNotice m_{T2} calculation is done with MADANALYSIS 5 function ($PHYSICS \rightarrow Transverse \rightarrow MT2(vec1, vec2, E_T^{miss}, m_{invisible})$)

and (280, 1) GeV are used in this note to illustrate the validation of our reimplementation. We make use of MADGRAPH5 aMC@NLO version 2.6.7¹⁰ for hard-scattering event generation in which leading-order matrix elements are convoluted with the NNPDF23LO¹¹ parton distribution function (PDF) set. The signal includes the emission of up to two additional partons. We apply the MLM scheme^{12,13} of the ME-PS matching with $xqcut = m_{\tilde{\tau}}/4$. The PYTHIA8 version 8.244¹⁴ with A14 tune has been used for the simulation of the parton showering and hadronization. The simulation of the detector response has been performed by using DELPHES-3.4.2,¹⁵ that relies on FASTJET¹⁶ for object reconstruction. The modified delphes card has been used with an appropriate tuned detector card. For example, the loosened isolation criteria are applied to cover all offline object definitions. And the radius parameter of jet and minimum transverse momentum are lowered to 0.4 and 15 GeV with updating b and tau tagging efficiencies. Also, UniqueObjectFinder is disabled for overlap removal which is done in MADANALYSIS5. Finally, we have used the MADANALYSIS5 reimplementation to calculate the signal selection efficiencies.

3.2. Comparison with the official results

In Table 2 and 3, we compare the results obtained with our implementation to the official raw event numbers in the auxiliary tables provided by the ATLAS collaboration for the benchmark points with masses $m(\tilde{\tau}, \tilde{\chi}_1^0) = (120, 1)$ and (280, 1) GeV, respectively. For each cut, we have calculated the related efficiency defined as

$$\epsilon_i = \frac{n_i}{n_{i-1}} \quad (14)$$

where n_i and n_{i-1} mean the event number after and before the considered cut, respectively. On the other hand, we have also calculated the differences between $\epsilon_i(MA5)$ and $\epsilon_i(ATLAS)$ with the definition as

$$diff. = \frac{\epsilon_i(MA5) - \epsilon_i(ATLAS)}{\epsilon_i(ATLAS)} \quad (15)$$

We observe that the disagreement on a cut-by-cut basis, is **195.4% and 215.4%** with all cuts for SR-lowMass and SR-highMass in Table 2 of $m(\tilde{\tau}, \tilde{\chi}_1^0) = (120, 1)$ GeV. The major parts of the disagreement come from **Trigger and offline cuts**, **2 medium τ (OS)** and **3rd baseline τ veto**, and **m_{T2} cut** steps. By lack of more public experimental information, we have not been able to validate these two steps more precisely.

In Fig. 2, we realize the m_{T2} distributions from ATLAS analysis are softer than our results. This causes the $m_{T2} > 70$ GeV cut looser in our reimplementation than the original ATLAS results which is taken from HEPData.⁶ Similarly, the disagreement on a cut-by-cut basis is **80.79% and 108.04%** with all cuts for SR-lowMass and SR-highMass in Table 3 of $m(\tilde{\tau}, \tilde{\chi}_1^0) = (280, 1)$ GeV. Again, the major parts of the disagreement come from **Trigger and offline cuts**, **2 medium τ (OS)**

6 *Jongwon Lim, Chih-Ting Lu, Jae-hyeon Park, and Jiwon Park*

Table 2. Validation checks of the cut flows for $\tilde{\tau}\tilde{\tau}$ production with $m(\tilde{\tau}, \tilde{\chi}_1^0) = (120, 1)$ GeV.

$\tilde{\tau}\tilde{\tau}$ production with $m(\tilde{\tau}, \tilde{\chi}_1^0) = (120, 1)$ GeV					
	ATLAS(N_{raw})	ϵ_i (%)	MA5(N_{raw})	ϵ_i (%)	diff.(%)
Generator filter	410000		922987		
Baseline cut	43062	10.5	27758	3.0	-71.43
SR-low Mass					
Trigger and offline cuts	10324	23.97	8836.8	31.84	30.84
2 medium τ (OS) and 3rd medium τ veto	6660	64.51	8224.8	93.07	44.27
b -jet veto	6554	98.41	8040.8	97.76	-0.66
Light lepton veto	6543	99.83	8035.2	99.93	0.10
Z/H -veto	6512	99.53	7978.4	99.29	-0.24
$75 < E_T^{miss} < 150$ GeV	2228	34.21	2777.6	34.81	1.75
2 tight τ	1565	70.24	1951	70.24	0.0
$ \Delta\phi(\tau; \tau) > 0.8$	1564	99.94	1946	99.74	-0.2
$ \Delta R(\tau; \tau) < 3.2$	1429	91.37	1783	91.62	0.27
$m_{T2} > 70$ GeV	280	19.59	531.6	28.81	47.06
All		0.65		1.92	195.4
SR-high Mass					
Trigger and offline cuts	2283	5.30	2096	7.55	42.45
2 medium τ (OS) and 3rd medium τ veto	1457	63.82	1896.8	90.50	41.81
b -jet veto	1407	98.07	1812	95.53	-2.59
Light lepton veto	1404	99.79	1808.8	99.82	0.03
Z/H -veto	1272	90.60	1671.2	92.39	1.98
≥ 1 tight τ	1249	98.19	1627.4	97.38	-0.82
$ \Delta\phi(\tau; \tau) > 0.8$	1236	98.96	1596.2	98.08	-0.89
$ \Delta R(\tau; \tau) < 3.2$	1132	91.59	1438.9	90.15	-1.57
$m_{T2} > 70$ GeV	170	15.02	342.8	23.82	58.59
All		0.39		1.23	215.4

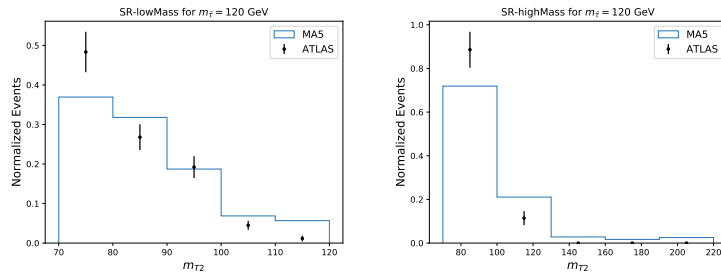
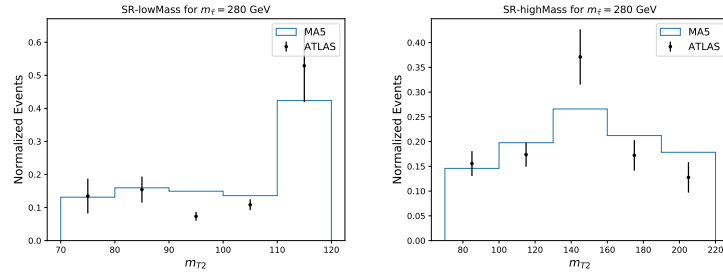


Fig. 2. The m_{T2} distributions for $m(\tilde{\tau}, \tilde{\chi}_1^0) = (120, 1)$ GeV.

and 3rd medium τ veto, and m_{T2} cut steps. The m_{T2} distributions are shown in Fig. 3 for the comparison of our results with ATLAS analysis.

Table 3. Validation checks of the cut flows for $\tilde{\tau}\tilde{\tau}$ production with $m(\tilde{\tau}, \tilde{\chi}_1^0) = (280, 1)$ GeV.

$\tilde{\tau}\tilde{\tau}$ production with $m(\tilde{\tau}, \tilde{\chi}_1^0) = (280, 1)$ GeV					
	ATLAS(N_{raw})	ϵ_i (%)	MA5(N_{raw})	ϵ_i (%)	diff.(%)
Generator filter	42000		578102		
Baseline cut	7312	17.41	37397	6.47	-62.84
SR-low Mass					
Trigger and offline cuts	3116	42.61	20308.8	54.31	27.46
2 medium τ (OS) and 3rd baseline τ veto	2036	65.34	19089.6	94.00	43.86
b -jet veto	1997	98.08	18577.6	97.32	-0.77
Light lepton veto	1988	99.55	18565.6	99.94	0.39
Z/H -veto	1920	96.58	17984.8	96.87	0.30
$75 < E_T^{miss} < 150$ GeV	738	38.44	6522.4	36.27	-5.65
2 tight τ	512	69.38	4581.5	70.24	1.24
$ \Delta\phi(\tau; \tau) > 0.8$	512	100.00	4551.1	99.34	-0.66
$ \Delta R(\tau; \tau) < 3.2$	478	93.36	4148.8	91.16	-2.36
$m_{T2} > 70$ GeV	278	58.16	2568	61.90	6.43
All		3.80		6.87	80.79
SR-high Mass					
Trigger and offline cuts	1973	26.98	13557.6	36.25	34.36
2 medium τ (OS) and 3rd baseline τ veto	1276	64.67	12630.4	93.16	44.05
b -jet veto	1244	97.49	12234.4	96.86	-0.65
Light lepton veto	1239	99.60	12223.2	99.91	0.31
Z/H -veto	1096	88.46	10865.6	88.89	0.49
≥ 1 tight τ	1076	98.18	10580.8	97.38	-0.81
$ \Delta\phi(\tau; \tau) > 0.8$	1045	97.12	10138.3	95.82	-1.33
$ \Delta R(\tau; \tau) < 3.2$	973	93.11	9482.4	93.53	0.45
$m_{T2} > 70$ GeV	691	71.02	7352.5	77.54	9.18
All		9.45		19.66	108.04

Fig. 3. The m_{T2} distributions for $m(\tilde{\tau}, \tilde{\chi}_1^0) = (280, 1)$ GeV.

4. Conclusions

We have implemented the ATLAS-SUSY-2018-04 search in the MADANALYSIS 5 framework. Our analysis has been validated in the context of a supersymmetry-inspired simplified benchmark model in which the Standard Model is extended by a neutralino and a stau decaying into a tau lepton and a neutralino, employing two

8 *Jongwon Lim, Chih-Ting Lu, Jae-hyeon Park, and Jiwon Park*

different benchmark points in the parameter space. By comparing our predictions for the cutflow with the official one provided by ATLAS in Ref.,⁵ we have found an agreement for each step in Table 2 and 3 except for the ones from **Trigger and offline cuts, 2 medium τ (OS) and 3rd medium τ veto**, and m_{T2} cut. Due to the lack of more information, we have not been able to validate these steps more precisely.

Acknowledgments

Dedications and funding information may be included here.

References

1. E. Conte and B. Fuks, *Int. J. Mod. Phys. A* **33** (2018) no.28, 1830027 [arXiv:1808.00480 [hep-ph]].
2. B. Dumont *et al.*, *Eur. Phys. J. C* **75** (2015) no.2, 56 [arXiv:1407.3278 [hep-ph]].
3. E. Conte, B. Dumont, B. Fuks and C. Wymant, *Eur. Phys. J. C* **74** (2014) no.10, 3103 [arXiv:1405.3982 [hep-ph]].
4. E. Conte, B. Fuks and G. Serret, *Comput. Phys. Commun.* **184** (2013) 222 [arXiv:1206.1599 [hep-ph]].
5. G. Aad *et al.* [ATLAS Collaboration], *Phys. Rev. D* **101**, no. 3, 032009 (2020) doi:10.1103/PhysRevD.101.032009 [arXiv:1911.06660 [hep-ex]].
6. G. Aad *et al.* [ATLAS], doi:10.17182/hepdata.92006
7. M. Cacciari, G. P. Salam and G. Soyez, *JHEP* **0804**, 063 (2008) doi:10.1088/1126-6708/2008/04/063 [arXiv:0802.1189 [hep-ph]].
8. C. Duhr and B. Fuks, *Comput. Phys. Commun.* **182**, 2404 (2011) doi:10.1016/j.cpc.2011.06.009 [arXiv:1102.4191 [hep-ph]].
9. A. Alloul, N. D. Christensen, C. Degrande, C. Duhr and B. Fuks, *Comput. Phys. Commun.* **185**, 2250 (2014) doi:10.1016/j.cpc.2014.04.012 [arXiv:1310.1921 [hep-ph]].
10. J. Alwall *et al.*, *JHEP* **1407**, 079 (2014) doi:10.1007/JHEP07(2014)079 [arXiv:1405.0301 [hep-ph]].
11. A. D. Martin, W. J. Stirling, R. S. Thorne and G. Watt, *Eur. Phys. J. C* **63**, 189 (2009) doi:10.1140/epjc/s10052-009-1072-5 [arXiv:0901.0002 [hep-ph]].
12. M. L. Mangano, M. Moretti, F. Piccinini and M. Treccani, *JHEP* **0701**, 013 (2007) doi:10.1088/1126-6708/2007/01/013 [hep-ph/0611129].
13. J. Alwall, S. de Visscher and F. Maltoni, *JHEP* **0902**, 017 (2009) doi:10.1088/1126-6708/2009/02/017 [arXiv:0810.5350 [hep-ph]].
14. T. Sjostrand, S. Mrenna and P. Z. Skands, *Comput. Phys. Commun.* **178**, 852 (2008) doi:10.1016/j.cpc.2008.01.036 [arXiv:0710.3820 [hep-ph]].
15. J. de Favereau *et al.* [DELPHES 3 Collaboration], *JHEP* **1402**, 057 (2014) doi:10.1007/JHEP02(2014)057 [arXiv:1307.6346 [hep-ex]].
16. M. Cacciari, G. P. Salam and G. Soyez, *Eur. Phys. J. C* **72**, 1896 (2012) doi:10.1140/epjc/s10052-012-1896-2 [arXiv:1111.6097 [hep-ph]].